

---

## Chapter 4 Specific heat studies on BiFeO<sub>3</sub> and its solid solution with BaTiO<sub>3</sub>

---

### 4.1. Introduction

Ever since its discovery in 1970's, studies on spin-glass (SG) transitions continue to receive tremendous interest in condensed matter and materials physics, till date [24,41,42,123,271–278]. The SG transition in the dilute magnetic systems has been the focus of initial studies in the field leading to development of theoretical tools to capture the essential physics underlying history dependent effects, divergence of third order ( $\chi_3$ ) non-linear susceptibility, critical slowing down of spin dynamics and ergodicity breaking, extremely slow non-Debye relaxation of magnetization on switching off the field [24,41,42,198,262,271], and memory and rejuvenation effects [198,279]. In this context, the role of frustrated interactions and randomness due to disorder has been identified as the key ingredients leading to SG states. A similar approach for concentrated magnetic systems, especially for compositions near the percolation threshold, predict coexistence of long-range ordered (LRO) and SG phases for both Ising and Heisenberg spins [24,42]. As discussed in the previous chapter, the experimental verification of such a coexistence has been quite controversial as similar phenomenon can also occur due to extrinsic factors like phase separation and segregation of impurities [171,238,239,242,243]. As a result, the initial reports on re-entrant SG transition below the LRO FM/AFM transition temperature ( $T_c/T_N$ ) were taken with disbelief [171,238,239,242,243]. It is generally believed that the intrinsic nature of such a phase coexistence cannot be verified using macroscopic measurements alone and require microscopic probes such as neutron scattering, muon spin rotation ( $\mu$ SR) and Mössbauer technique [172]. In the preceding chapter, we showed using neutron scattering measurements that in disordered BiFeO<sub>3</sub>, such a phase coexistence occurs due to the

detachment of small longitudinal/transverse components of the  $3d\text{Fe}^{3+}$  spins from the LRO phase which freeze into the SG state. More interestingly, we demonstrated for the first time that SG transitions in such disordered multiferroics is accompanied with magnetoelectric and magnetoelastic couplings leading to change in ferroelectric polarization and unit cell volume, respectively. In this chapter, we use specific heat measurements to provide additional evidence for the coexistence of LRO AFM and SG phases at low temperatures.

Specific heat studies have been very useful in studying the role of electrons, phonons, magnons, Schottky defect, hyperfine splitting etc. to the total specific heat measured experimentally in various types of phase transitions, especially in ferroics and multiferroics [24,42,60–62,280,281]. In the context of SG transition, a characteristic linear dependence of the magnetic contribution to the specific heat ( $C_m$ ) below the SG freezing temperature  $T_f$  was reported experimentally [42,55–57,282,283] and explained theoretically using two level tunnelling model in dilute systems [54,284]. In concentrated systems, there is no unanimity about the temperature dependence of the magnetic contribution to the specific heat below  $T_f$ . Different empirical and theoretical models involving linear [55–57], exponential [58–62] and power law [63,64] type dependence of magnetic contribution to the specific heat have been proposed in the literature for the concentrated systems. Although most of these specific heat studies on concentrated systems are on compositions which show coexistence of LRO and SG phases, the low temperature specific heat behaviour has been modelled as if the entire contribution to the magnetic contribution  $C_m$  is essentially due to the SG phase only. The present investigation was undertaken to seek the signatures of phase coexistence in the temperature dependence of specific heat of  $(\text{Bi}_{1-x}\text{Ba}_x)(\text{Fe}_{1-x}\text{Ti}_x)\text{O}_3$  [BF-xBT] system where coexistence of the LRO AFM phase with SG phase was established using

macroscopic as well as microscopic probes as described in the preceding chapter (chapter-III). We show here that the low temperature behaviour of the magnetic contribution to the specific heat below the Boson peak ( $C_p/T^3$  versus T plot) temperature cannot be modelled using SG phase exclusively. We also show that the coexistence model explains the low temperature specific heat behaviour quite precisely. We believe that this is the first evidence for the coexistence of LRO and SG phases in a concentrated system using specific heat studies.

## **4.2. Sample preparation and characterization details:**

Polycrystalline samples of  $(\text{Bi}_{1-x}\text{Ba}_x)(\text{Fe}_{1-x}\text{Ti}_x)\text{O}_3$  or BF-xBT with  $x = 0.0$  to  $0.60$  at a step of  $0.10$  prepared by standard solid-state route using high purity oxides were used in this study. The details of sample preparation and characterizations are given in the preceding two chapters. The specific heat at constant pressure ( $C_p$ ) was measured using a physical properties measurement system (PPMS) (Dynacool, Quantum Design). The thermal relaxation of calorimeter is employed to extract the value of specific heat. A small piece of the sintered pellet ( $\sim 12\text{mg}$ ) with smooth surface is attached to the specific heat platform using apiezone N-grease. Before each sample measurement, measurement was carried out on the addenda (platform + apiezone N-grease) also. The apiezone N-grease is used for better thermal conduction between sample and platform of the puck. The absolute value of the specific heat of sample was obtained by subtracting the value of specific heat of addenda from the total measured specific heat.

## **4.3. Results and discussion:**

### **4.3.1 Different contributions to total specific heat:**

It is well established that the measured total specific heat of a material at constant pressure has various contributions which can be expressed as [280]:

$$C_{\text{total}} = C_{\text{electronic}} + C_{\text{phonon}} + C_{\text{magnon}} + C_{\text{spin-glass}} + C_{\text{hyperfine splitting/schottky}}$$

The electronic and phonon contributions are of non-magnetic origin and are given by the Eqs. (4.1) and (4.2) below [280]:

$$C_{\text{electronic}} = \gamma T \quad \dots\dots\dots (4.1)$$

and

$$C_{\text{phonon}} = 9N_A k_B \left(\frac{T}{\Theta_D}\right)^3 \int_0^{\Theta_D/T} \frac{x^4 e^x}{(e^x - 1)^2} dx, \quad \dots\dots\dots(4.2)$$

Here,  $N_A$  is the Avogadro number,  $k_B$  is the Boltzmann constant,  $\Theta_D$  the Debye temperature and  $x = \hbar\omega/k_B T$ , where  $\hbar$  is the Planck's constant and  $\omega$  the phonon frequency.

The magnon contribution to specific heat for antiferromagnetic ordering is given by [280]:

$$C_{\text{magnetic}} = \frac{4\pi k_B^4}{(\gamma D \hbar)^3 \hbar} T^3 \int_0^{\Theta_m/T} \frac{x^3}{e^x - 1} dx \quad \dots\dots\dots(4.3)$$

where  $x = \hbar\omega/k_B T$ ,  $\gamma$  is Gyromagnetic ratio and  $D$  is proportionality constant.

The hyperfine splitting/Schottky contribution is usually modelled as [281]:

$$C_{\text{hyperfine splitting/Schottky}} = \frac{R}{T^2} \frac{\sum_i \sum_j (\Delta_i^2 - \Delta_i \Delta_j) \exp[-(\Delta_i + \Delta_j)/T]}{\sum_i \sum_j \exp[-(\Delta_i + \Delta_j)/T]} \quad \dots\dots(4.4)$$

where  $\Delta_i = \varepsilon_i/k_B$  and  $\varepsilon_i$  is  $i^{\text{th}}$  energy level,  $R$  is universal gas constant ( $8.314 \text{ Jmol}^{-1} \text{ K}^{-1}$ ).

The hyperfine splitting or nuclear contribution may be neglected in our case as it is known to dominate at very low temperatures (i.e. millikelvin range) whereas our data is from 1.8K to 300K. Low temperature measurements in the millikelvin temperature range is needed to precisely determine whether it is present or not in BF-xBT samples. Further, our samples are insulators, so the electronic contribution to specific heat can also be

neglected. So, we shall focus on the phonon, antiferromagnetic magnon and glassy contributions to the specific heat.

The magnetic contribution ( $C_m$ ) to the specific heat for long-range ordered (LRO) ferromagnetic (FM)/antiferromagnetic (AFM) magnons at low temperatures varies as  $C_m \sim T^{d/n}$ , where  $d$  is the dimensionality and  $n$  is the exponent of wave vector  $k$  in the magnon dispersion curve. Typically, LRO AFM and LRO FM states give  $T^3$  and  $T^{3/2}$  type dependence at low temperatures. Moreover, detailed calculations by Cooper and Mackintosh [58] have shown that some magnetic contributions to specific heat may also follow exponential behaviour at low temperatures  $C_m = f(T)\exp(-\Delta E/k_B T)$ , where  $\Delta E$  is an energy gap. This type of exponential behaviour has been attributed to the gapped magnons which can arise due to D-M interaction and single-ion anisotropies [58] and have been postulated in spin glasses also [59–62].

As said earlier, for dilute spin-glass systems, a characteristic linear dependence of the magnetic contribution to the specific heat below the SG freezing temperature  $T_f$  has been observed experimentally and explained theoretically using two level tunnelling model [54]. For concentrated systems, different empirical and theoretical models of magnetic contribution to the specific heat have been proposed in the literature. (1) linear temperature dependence of  $C_m$  below  $T_f$  [55–57], (2)  $C_m$  modelled using exponential functions ( $C_m = aT^{1/2}\exp(-\Delta E/k_B T)$ ,  $C_m = aT\exp(-\Delta E/k_B T)$ ,  $C_m = aT^{-2}\exp(-\Delta E/k_B T)$ ) [58–62] and (3)  $C_m$  modelled by a power law  $C_m \sim T^\alpha$ , where  $\alpha = 1.2$  to  $2$  at low temperatures [63,64]. Power law has been mostly used for geometrically frustrated AFM systems.

Before proceeding to model the low temperature behaviour of magnetic contribution ( $C_m$ ) to the total specific heat ( $C_p$ ) of BF-xBT for spin-glass and LRO AFM contributions, it is worth summarizing the status of the modelling of  $C_m$  behaviour at low

temperatures in dilute and concentrated spin-glass systems. In the canonical (dilute) spin-glass systems, like CuMn, AuFe, the magnetic contribution to specific heat shows linear dependence at low temperature and a broad maximum above the spin glass freezing temperature  $T_f$  at nearly 1.5 times the freezing temperature ( $1.5T_f$ ). No anomaly is observed in the vicinity of  $T_f$  [41]. The numerical calculations by Walker and Walstedt [285] have also confirmed this linear dependence of  $C_m$  in dilute (metallic) spin-glass systems [282]. The concentrated cluster spin glass systems, like  $\text{Eu}_x\text{Sr}_{1-x}\text{S}$  ( $x = 0.40, 0.54$ ), display smeared rounded peak in  $C_m$  around  $T \sim 2T_f$ , and the decrease in  $C_m$  is faster than the canonical (dilute) spin glass systems. Towards higher temperature side, the magnetic specific heat data of CuMn roughly follows  $1/T$  dependence as expected on the basis of scaling theories [282] while in cluster spin-glass systems, the thermal disorder rapidly destroys the short-range magnetic ordering and thus leads to faster return of the  $C_m$  value to zero [55,56]. For  $\text{Eu}_x\text{Sr}_{1-x}\text{S}$  with  $x = 0.40$ , the lattice contribution is less than 0.3 % of the measured specific heat below 10K and hence negligible [56]. These compositions are reported to display the characteristic spin-glass type linear variation of  $C_m$  with temperature below  $T_f$ , a broad maximum well above  $T_f$  and no singularity at  $T_f$ . However, at very low temperatures (below 0.45K) a distinct deviation from this linear behaviour is observed and the data is adequately represented by  $C_m = AT + B/T^2$  type function [55,56]. The first term is the well-known spin-glass term and the second term  $B/T^2$  is due to the Schottky anomaly or hyperfine splitting of the  $^{151}\text{Eu}$  and  $^{153}\text{Eu}$  nuclei [55,56]. However, in the presence of field (1T), the low temperature spin-glass phase is suppressed and induces a ferromagnetic ordering [55]. For  $x = 0.54$ , a deviation of spin-glass specific heat from strictly linear behaviour is observed for  $T < T_f$ . A better fit has been reported by adding a  $T^2$  term:  $C_m = AT + B/T^2 + CT^2$  [55,56]. Such a  $T^2$  term has been frequently used to describe the small deviation from the linear dependence [55,56].

The most convincing interpretation of the  $C_m$  at low temperatures in  $\text{Eu}_x\text{Sr}_{1-x}\text{As}_3$  with  $x=0.24$  and  $x=0.30$ , showing freezing of the transverse and longitudinal components at successively lower temperatures, like BF-xBT discussed in the previous chapter, has been found in terms of an exponential function  $C_m = aT \exp(-\Delta E/k_B T)$  corresponding to a gapped magnon [58–62].

### 4.3.2 Low temperature specific heat behaviour of BF-xBT:

After setting the necessary background, we now proceed to discuss our experimental observations. In order to probe the nature of ground state and magnetic transitions in the multiferroic BF-xBT system with  $x = 0.0$  to  $0.60$ , we carried out specific heat measurements under zero-magnetic field in the temperature range  $1.8$ - $300$  K and the results are shown in Fig. 4.1. We first examine the data qualitatively towards the higher temperature side. As per Dulong-Petit law, the value of specific heat at constant volume ( $C_v$ ) having  $n$  atoms per formula unit should approach asymptotically the value  $3nR$  J/mol-K, where  $R$  is the gas constant. In our case  $n = 5$  and therefore the maximum value of  $C_v$  is  $\sim 124.7$  J/mol-K. Further, the specific heat at constant pressure ( $C_p$ ) is always higher than the specific heat at constant volume which should approach  $3nR$  J/mol-K well above the Debye temperature ( $\Theta_D$ ). Our  $C_p$  data shown in Fig. 4.1 for  $x = 0, 0.10$ , and  $0.20$  are consistent with the expected behaviour. It is also in excellent agreement with the reported values measured experimentally and predicted theoretically for pure ( $x = 0$ )  $\text{BiFeO}_3$  [286–289].

Towards understanding the phase transition and true ground state of the multiferroic system BF-xBT using specific heat measurements, there are challenges in separating out the phonon contributions from the total specific heat. There is no standard protocol to subtract the phonon contributions to obtain the magnetic specific heat. For

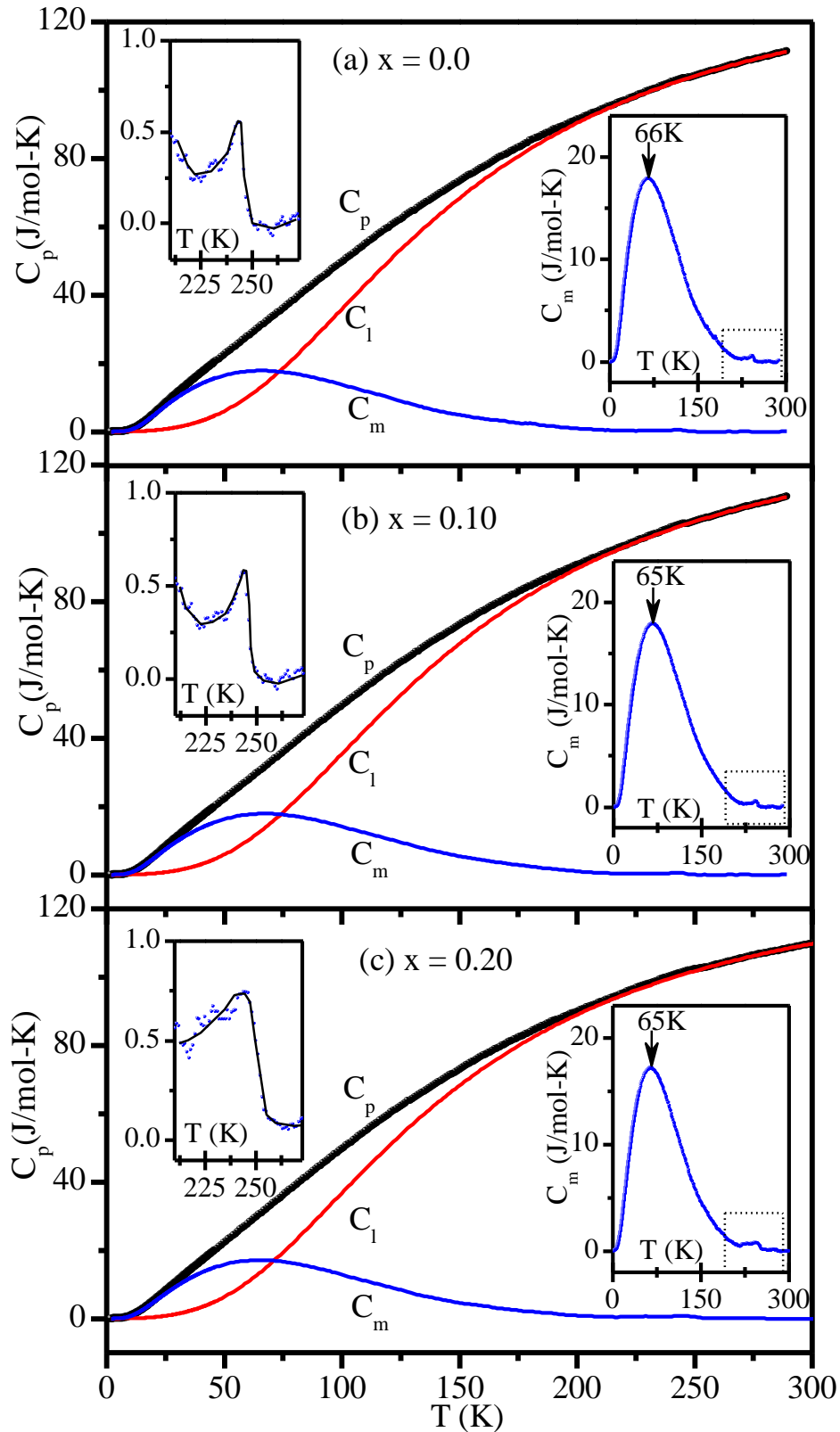


Figure 4.1: Temperature dependence of total specific heat ( $C_p$ ), phonon contribution ( $C_l$ ) and magnetic contribution ( $C_m$ ) of BF-xBT for (a)  $x = 0$  (b)  $x = 0.10$  and (c)  $x = 0.20$ .

BF-xBT system, there is also no non-magnetic analogue which has identical crystal structure and whose specific heat can be used to subtract the phonon contribution for obtaining the magnetic contribution as has been done in some other systems. Further, this subtraction becomes a nearly impossible task with antiferromagnetic long-range ordering as both the phonon and magnon contributions have the same  $T^3$  dependence at low temperatures. To the best of our knowledge, no specific heat study has been performed on BF-xBT system, except for  $x = 0$  [286–289], in the literature. Further, no attempt has been made to separate out the magnetic contribution. In order to subtract the phonon contribution, we used the Debye temperature ( $\Theta_D$ ), determined from the thermal expansion data discussed in chapter III, as the initial input value for obtaining the most plausible value of  $\Theta_D$  through successive refinements until a self-consistent value of  $\Theta_D$  was obtained such that it explains the observed value of specific heat at high temperatures (260 to 295K range) and also gives  $T^3$  dependence at low temperatures as per Debye theory of specific heat. After the determination of the  $\Theta_D$ , we calculated the phonon contribution ( $C_l$ ) from 1.8K to 300K using the Debye expression given by Eq. (4.2). This is shown in Fig. 4.1 for BF, BF-0.10BT and BF-0.20BT samples along with the total specific heat. It can be seen from this figure that the calculated phonon contribution using Eq. (4.2) is in excellent agreement with the measured specific heat data towards higher temperature side. The best fit is obtained for  $\Theta_D = (609 \pm 10)K$ ,  $(607 \pm 10)K$ ,  $(585 \pm 10)K$  for BF, BF-0.10BT and BF-0.20BT samples. The best fit value for  $\text{BiFeO}_3$  ( $\Theta_D = 609 \pm 10$ ) is in close agreement with the reported value (577K) by Park et al. [82], determined from the thermal expansion behaviour of the XRD data, and also the predicted value by the density functional theory (DFT) calculations ( $\Theta_D = 554K$ ) [287]. The value obtained from thermal expansion data of BF-0.20BT in chapter III also falls in a similar range.

To obtain the magnetic contribution to specific heat  $C_m$ , we subtracted the calculated phonon/lattice contribution ( $C_l$ ) from total specific heat ( $C_p$ ). The magnetic contribution to the specific heat ( $C_m$ ) of BF, BF-0.10BT and BF-0.20BT so obtained is also shown in Fig 4.1. Two anomalies around 250K and 66K are clearly discernible in the magnetic contribution to the specific heat which we attribute to the two spin-glass phases SG1 and SG2. The peak around 66K in the  $C_m$  vs T plot is quite diffuse and rules out long-range magnetic ordering transition [42]. The absence of sharp peaks in the  $C_m$  is a well-known characteristic feature of the existence of disordered spin configurations [55,56,59].

Now we proceed to interpret the results of BF-xBT in the context of spin-glass phase in coexistence with the LRO AFM phase at low temperatures. It is well known that at very low temperatures, typically in the range 2-30K, several crystalline and glassy materials exhibit larger specific heat than predicted by Debye model. This excess specific heat manifests itself as a peak in the  $C_p/T^3$  versus T plot and is generally attributed to local low energy excitation modes observed in Raman spectra and inelastic neutron scattering [272,278,290–293]. This peak is called as Boson peak and has been observed in several glasses [272,278,290–293], both magnetic and non-magnetic. The strong Boson peak is observed in strong glasses and weak Boson peak occurs in fragile glasses [292]. Boson peak has also been attributed to Van Hove singularities where the vibrational density of states crosses the Debye density of states, leading to a flattening of the phonon dispersion curve [294]. As per Debye  $T^3$  law, the lattice contribution to  $C_p/T^3$  versus T plot should be constant at low temperatures. Therefore, the  $C_p/T^3$  vs T plot shown in Figs. 4.2 (a), (b), (c) and Fig. 4.3(b) for BF-xBT samples can be used to determine whether the Boson peak results from magnetic contributions or some other contributions present in the samples. The  $C_p/T^3$  vs T plot shown in Figs. 4.2(a), (b), (c) and Figs. 4.3 (b), reveals a

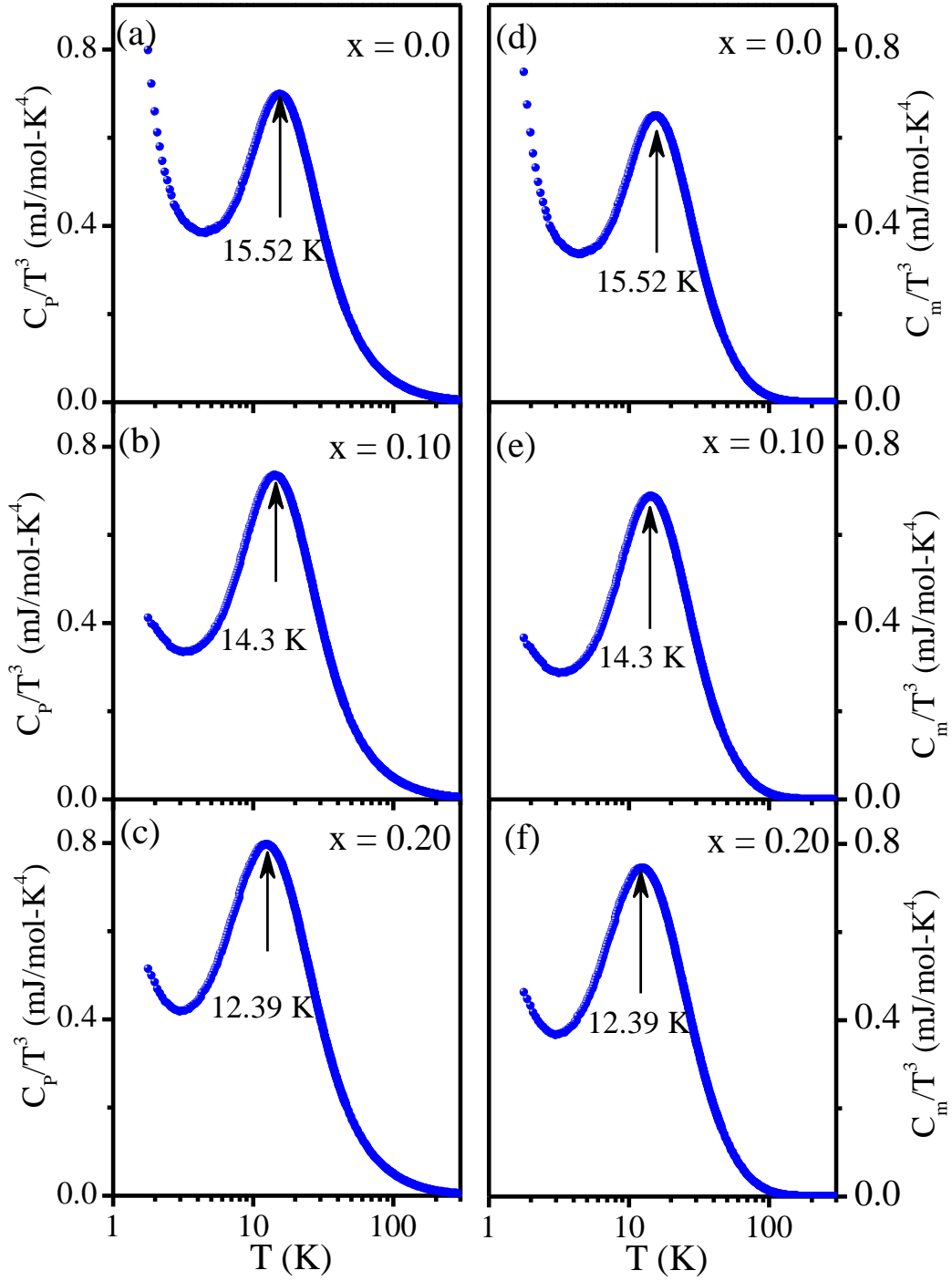


Figure 4.2: Left panel (a-c) shows the temperature evolution of Boson peak in the  $C_p/T^3$  versus  $T$  plot of BF- $x$ BT as a function of composition ( $x$ ). Right panel (d-f) depicts the temperature variation of magnetic Boson peak in the  $C_m/T^3$  versus  $T$  plot of BF- $x$ BT as a function of  $x$ .

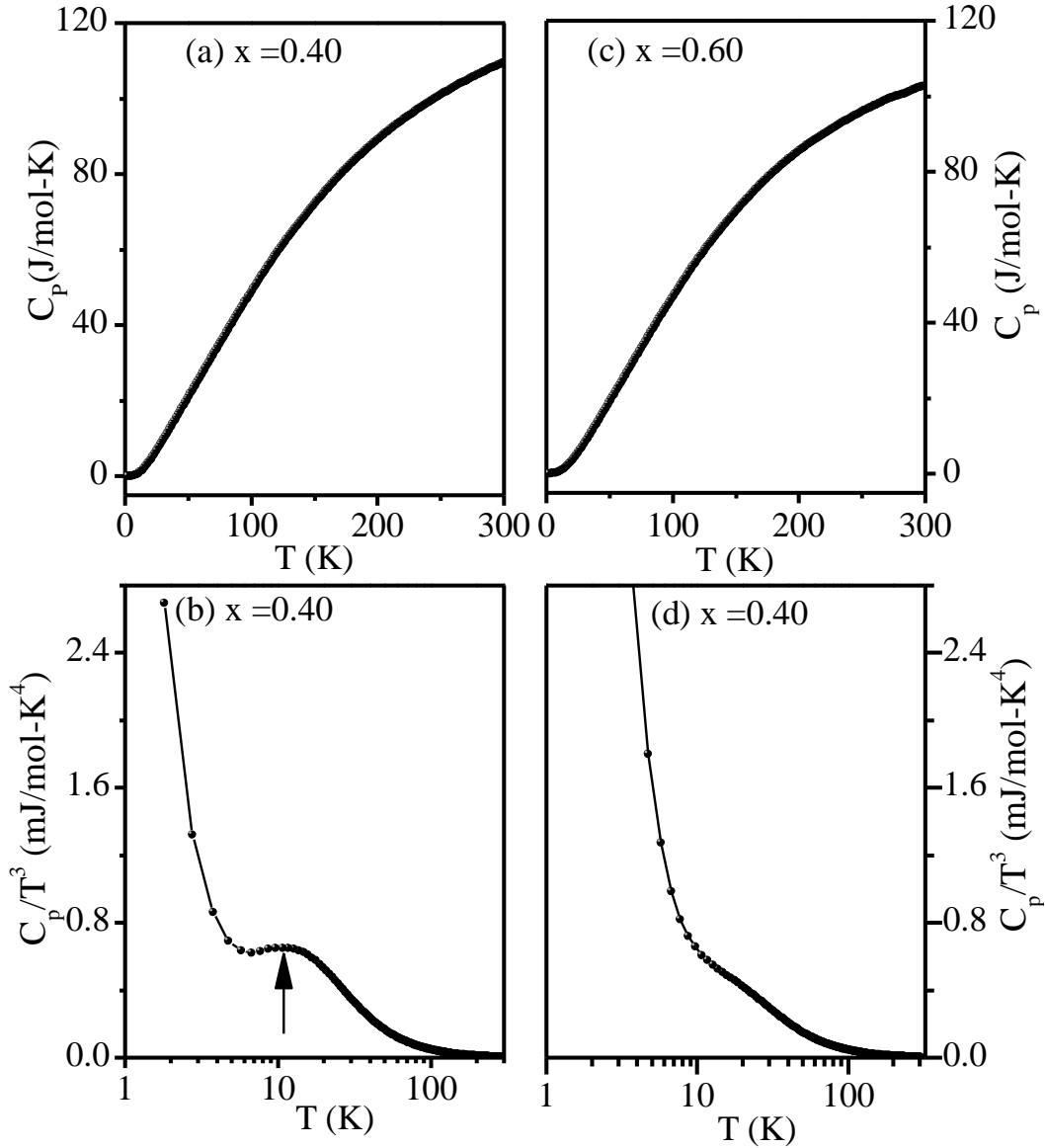


Figure 4.3: Left panel (a) and (b) shows the temperature dependence of total specific heat ( $C_p$ ) and Boson peak of BF-xBT for  $x = 0.40$ . Right panel (c) and (d) shows the temperature dependence of total specific heat ( $C_p$ ) and Boson peak for  $x = 0.60$ .

Boson peak around 15.52K, 14.3K, 12.39, and 9.64K for  $x = 0.0, 0.10, 0.20$  and  $0.40$ , respectively. For  $x = 0.60$ , the signature of Boson peak is too weak to be compared with other BF-xBT composition (see Fig. 4.3(d)). For this composition, we do not observe spin glass transition at low temperatures. Thus the existence of Boson peak in BF-xBT is clearly linked with the spin glass transition at low temperatures. It is interesting to note that even after subtracting the phonon contribution,

the plot of  $C_m/T^3$  vs  $T$  continues to show the Boson peak at the same peak temperature (see Figs. 4.2 (d), (e), and (f)). This suggests that this peak is predominantly of magnetic origin. The observation of Boson peak in  $C_m / T^3$  vs  $T$  plot of BF-xBT is close to the gapped magnon mode observed at 1.1 meV by inelastic neutron scattering studies on BiFeO<sub>3</sub> [237]. Boson peak has been reported in several spin glass systems below the spin-glass transition temperature [272,278,294], as is the case with BF-xBT compositions. It is important to note that in several spin-glass systems, the specific heat starts increasing again well below the Boson peak temperature. We have also observed such an increasing trend for BF-xBT as can be seen from Fig. 4.2. Interestingly, there is a small but systematic composition dependence of the Boson peak temperature and it follows  $T_{\text{Boson peak}} \sim (x-x_c)^n$  type dependence with an exponent  $n = 0.47 \pm 0.02$  for  $x_c = 0.55 \pm 0.01$  (see Fig. 4.4). The exponent being close to  $n = 1/2$  is reminiscent of a quantum phase transition and the possibility of the existence of a quantum critical point corresponding to the percolation threshold composition  $x_c = 0.55 \pm 0.01$  cannot be ruled out. But this aspect requires further investigation on several compositions close to  $x_c$ . Above  $x_c$ , neither LRO AFM nor spin-glass transitions are observed in BF-xBT system as can be seen from the phase diagram given in chapter III. We note that the exponent for the lower temperature spin-glass transition temperature is found to be  $n=0.08$  while the exponent for Boson peak corresponds to  $n=0.47 \pm 0.02$ . The reason for this difference is not obvious to us but may be due to the fact that  $T_f$  used in the phase diagram of chapter III was measured at 497.3 Hz. For spin-glasses this temperature is frequency dependent and  $T_f(\omega)$  in the limit of  $\omega$  tending towards zero is the real spin glass transition temperature  $T_{\text{SG}}$  below which the ergodicity symmetry is broken. The Boson peak temperature, on the otherhand, is not affected by frequency and may therefore be more reliable estimate for a characteristic temperature associated with the spin glass phase.

The temperature dependence of the magnetic contribution to specific heat ( $C_m$  vs  $T$  plot) for BF- $x$ BT shown in the insets of Fig. 4.1 for  $x = 0, 0.10,$  and  $0.20$  show features similar to those observed in concentrated insulating spin glasses. In case of BF- $x$ BT, the broad peak in  $C_m$  occurs at  $\sim 65$ K which corresponds to  $\sim 2T_f$ . The peak temperature 65K for  $C_m$  vs  $T$  plot corresponds to an energy gap of 6 meV reported by Lui et al. for BiFeO<sub>3</sub> [286]. The magnetic contribution starts decreasing above 65K but shows a small increase around 225K corresponding to the second spin-glass transition discussed in Chapter III. The small peak around 240K is relatively sharp in BiFeO<sub>3</sub> and BF-0.10BT but becomes diffuse for BF-0.20BT, as can be seen from the insets of Fig. 4.1, which depict this peak on a magnified scale. Because of the dominant contribution of phonons as compared to the magnons at high temperatures, no meaningful analysis could be

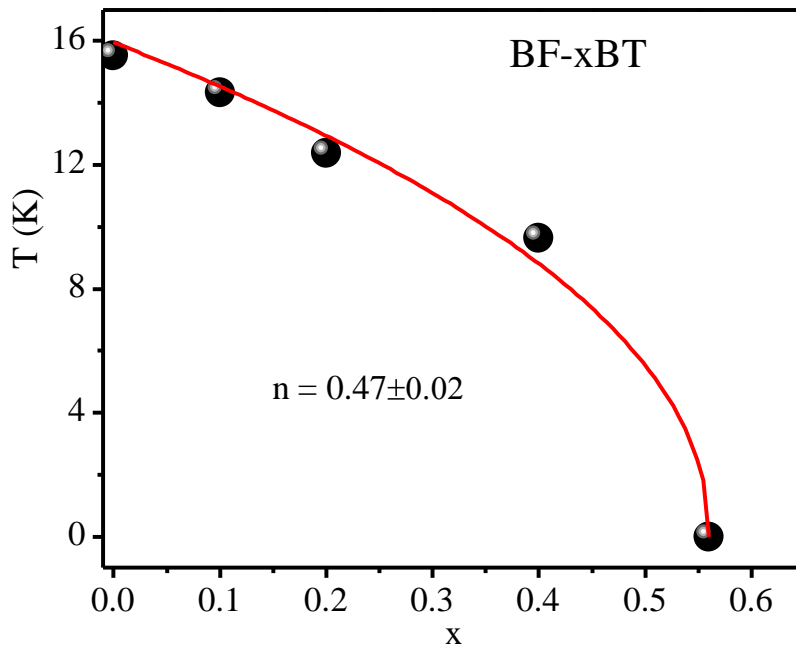


Figure 4.4: Variation of Boson peak temperature with composition. It follows  $(x-x_c)^{1/2}$  type dependence suggesting possibility of a quantum critical point at  $x_c \approx 0.55 \pm 0.01$ .

carried out for this anomaly except for noting that it has become diffuse for BF-0.20BT. On decreasing the temperature, the magnetic contribution starts increasing below 225K and peaks around 65K. We believe that this rapid increase in  $C_m$  is due to multimagnon contributions as has been noted in the context of pure BiFeO<sub>3</sub> also [286]. Raman scattering studies have revealed presence of magnon modes at 18 cm<sup>-1</sup> (25.8K), 22 cm<sup>-1</sup> (31.5K), 28cm<sup>-1</sup> (~40K) and 32cm<sup>-1</sup> (~46K) [111]. Further, inelastic neutron scattering studies have revealed two gapped magnons corresponding to 1.1±0.2 meV (~13K) and 2.5±0.2 meV (~29K) of which the latter is quite broad while the former is sharper [237]. Since there is a coexistence of LRO and SG phases in the ground state of BF-xBT, as discussed in chapter III, we have attempted to model the low temperature specific heat behaviour using both the contributions taking first BF-0.20BT composition. Figs. 4.5, 4.6 and 4.7 depict the magnetic part of specific heat in the temperature range 1.8-40K and the

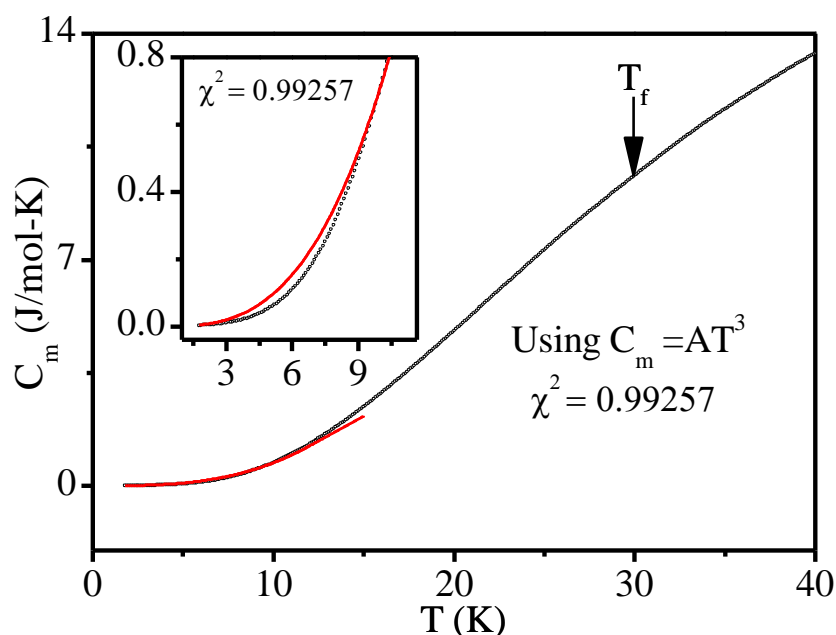


Figure 4.5: Temperature dependence of magnetic contribution to specific heat for BF-0.20BT in the range 1.8-40K. Solid line is the fit using  $AT^3$ -type dependence of  $C_m$ . Inset depicts the fit on a magnified scale.

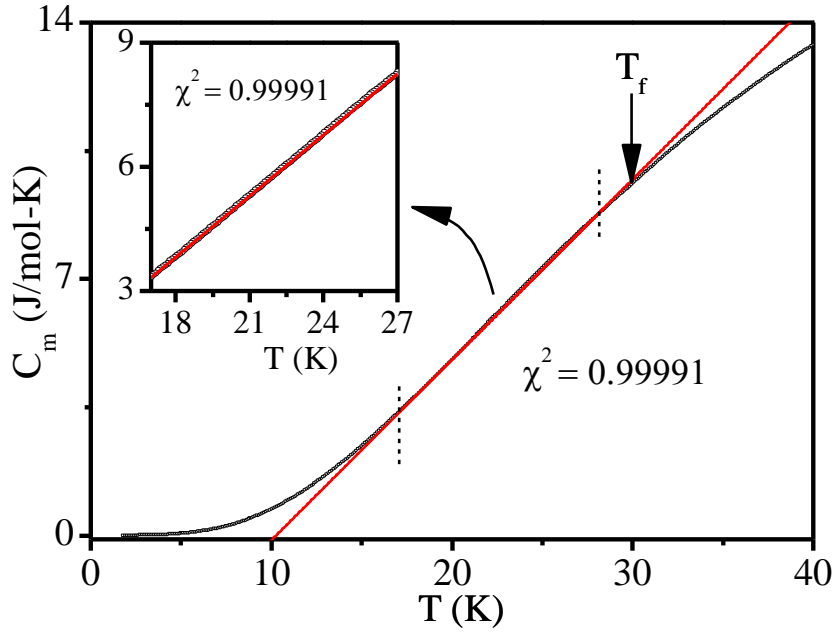


Figure 4.6: Temperature dependence of magnetic contribution to specific heat for BF-0.20BT in the range 1.8-40K. Solid line is the fit using  $C_m = AT$ -type dependence. Inset depicts the fit on a magnified scale.

fits using various models discussed in the previous section. It is found that the  $C_m$  cannot be modelled satisfactorily using LRO AFM magnon term ( $T^3$ ) alone. This can be seen from the fit shown in the inset of Fig. 4.5. This clearly suggests another contribution which we believe is of glassy origin. This is also corroborated by the fact that at low temperatures  $C_m/T^3$  vs  $T$  plot is not horizontal as expected for a typical AFM system (see Fig. 4.2(f)). It is found (not shown in the figure) that the fit between observed  $C_m$  and calculated  $C_m$  using  $T^3$  dependence in the 5 to 10K range becomes worse with increasing BT contribution. To model the spin glass contribution, we first considered the most widely used linear temperature dependence of  $C_m$  as reported in the dilute systems [282,283] and also in some concentrated systems [56,59,295]. In this context, we note that  $C_m$  indeed follows linear dependence below  $T_f$  in the temperature range  $\sim 17\text{K}$  to  $\sim 28\text{K}$  whose extrapolation cuts the temperature axis at  $\sim 10\text{K}$ , as shown in Fig. 4.6. However, this model cannot explain the specific heat behaviour below 17K. The

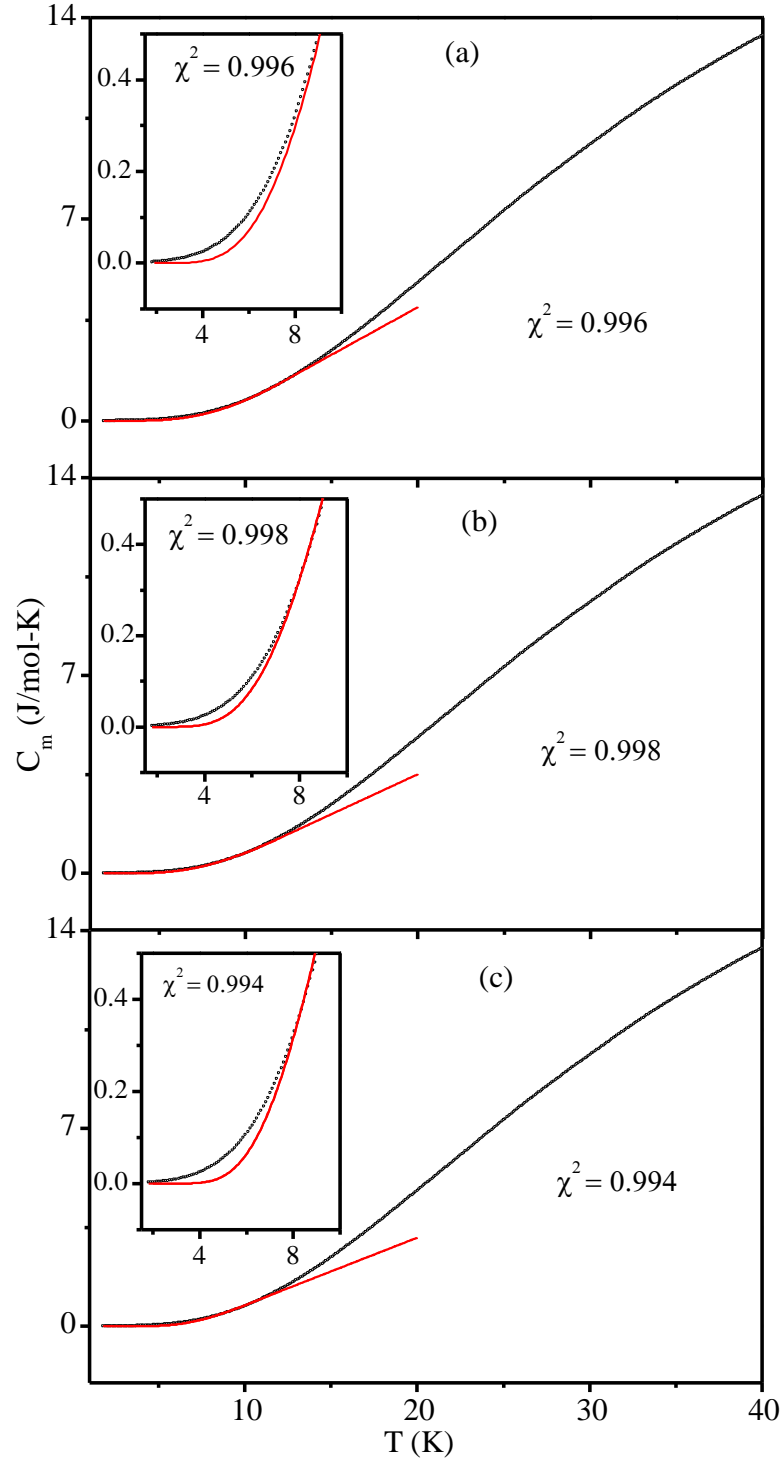


Figure 4.7: Temperature variation of magnetic contribution ( $C_m$ ) to specific heat for BF-0.20BT in the range 1.8 to 40K. Solid line is the fit corresponding to different model (a)  $C_m = aT^{1/2}\exp(-\Delta E/k_B T)$ , (b)  $C_m = aT\exp(-\Delta E/k_B T)$  (c)  $C_m = aT^2\exp(-\Delta E/k_B T)$  below the Boson peak temperature.

decrease in the  $C_m$  with temperature below 17K suggests exponential decay. Accordingly, we considered the following models used in the literature (i)  $C_m = aT^{1/2}\exp(-\Delta E/k_B T)$  [61], (ii)  $C_m = aT\exp(-\Delta E/k_B T)$  [58,59,61], (iii)  $C_m = aT^2\exp(-\Delta E/k_B T)$  [62], and the corresponding fits for BF-0.20BT below the Boson peak temperature (i.e., 1.8 to 12K range) are shown in Figs. 4.7 (a), (b) and (c), respectively. It is evident from the magnified views given in the insets of Fig. 4.7 that none of these models can provide satisfactory fit.

Since the low temperature specific heat behaviour in the 1.8 to 12K range cannot be modelled either by LRO AFM gapless magnon mode ( $C_m \sim T^3$ ) or by gapped magnon modes ( $C_m = f(T)\exp(-\Delta E/k_B T)$ ), we considered coexistence of LRO AFM and spin-glass phases. We tried all possible combinations, but the best fit was obtained for the following functional dependence  $C_m = AT^3 + B\exp(-\Delta E/k_B T)$ . The corresponding fit shown in Fig. 4.8(a) (see the inset for the quality of the fit) is excellent. For comparison, we also give a fit corresponding to  $C_m = AT^3 + BT$  type dependence in Fig. 4.8(b). This fit is rather poor as can be seen from the inset of Fig.4.8 (b) as compared to the fit shown in the inset of Fig 4.8(a). The fits for  $C_m$  versus  $T$  plots of BF and BF-0.10BT using  $C_m = AT^3 + B\exp(-\Delta E/k_B T)$  type dependence below the Boson peak temperature are shown in Fig. 4.9. The excellent quality of the fits can be seen from the insets of Fig. 4.9 where a magnified view is plotted. To summaries, the best and most reliable fit for the temperature dependence of the magnetic contribution to the specific heat of BF-xBT in the 1.8 to 12K range was obtained for  $C_m = AT^3 + B\exp(-\Delta E/k_B T)$  type functional dependence, where the first term is attributed to the LRO AFM magnons (gapless) and the second term is due to gapped magnons (non-propagating) of the SG phase [237]. This functional form gives gap energy of 3.1, 2.69, and 2.3 meV for  $x = 0, 0.10$  and  $0.20$ , respectively, The gap energy is close to the experimentally observed broad peak at  $\sim 2.5 \pm 0.2$  meV ( $\sim 29$ K) in

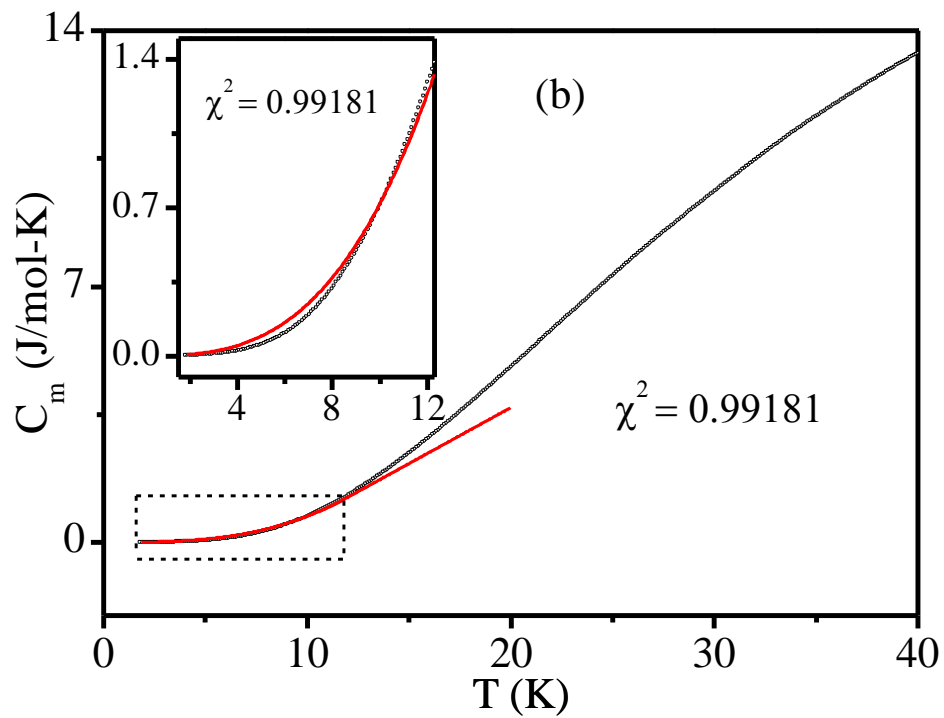
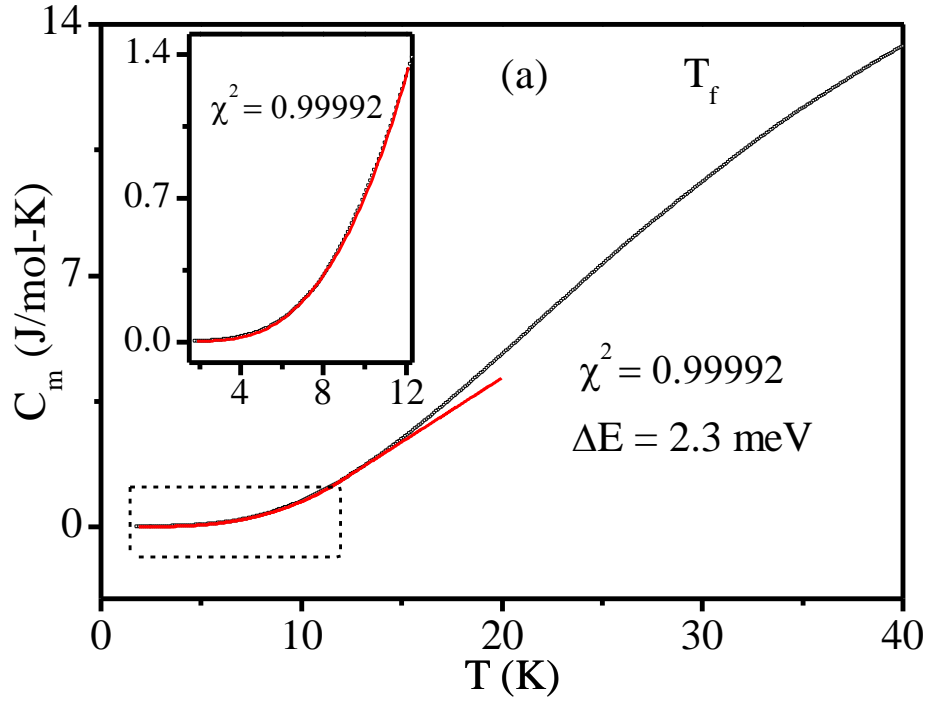


Figure 4.8: The fit to  $C_m$  versus  $T$  plot of BF-0.20BT using (a)  $C_m = AT^3 + B\text{exp}(-\Delta E/k_B T)$  and (b)  $C_m = AT^3 + BT$  type function dependence. The quality of the fits can be seen from the insets where a magnified view is plotted. In contrast,  $C_m = AT^3 + BT$  type dependence gives poor fit as can be seen from the inset of bottom panel (b) given on the left-hand corner. The goodness of fit  $\chi^2$  is better for the  $AT^3 + B\text{exp}(-\Delta E/k_B T)$  dependence.

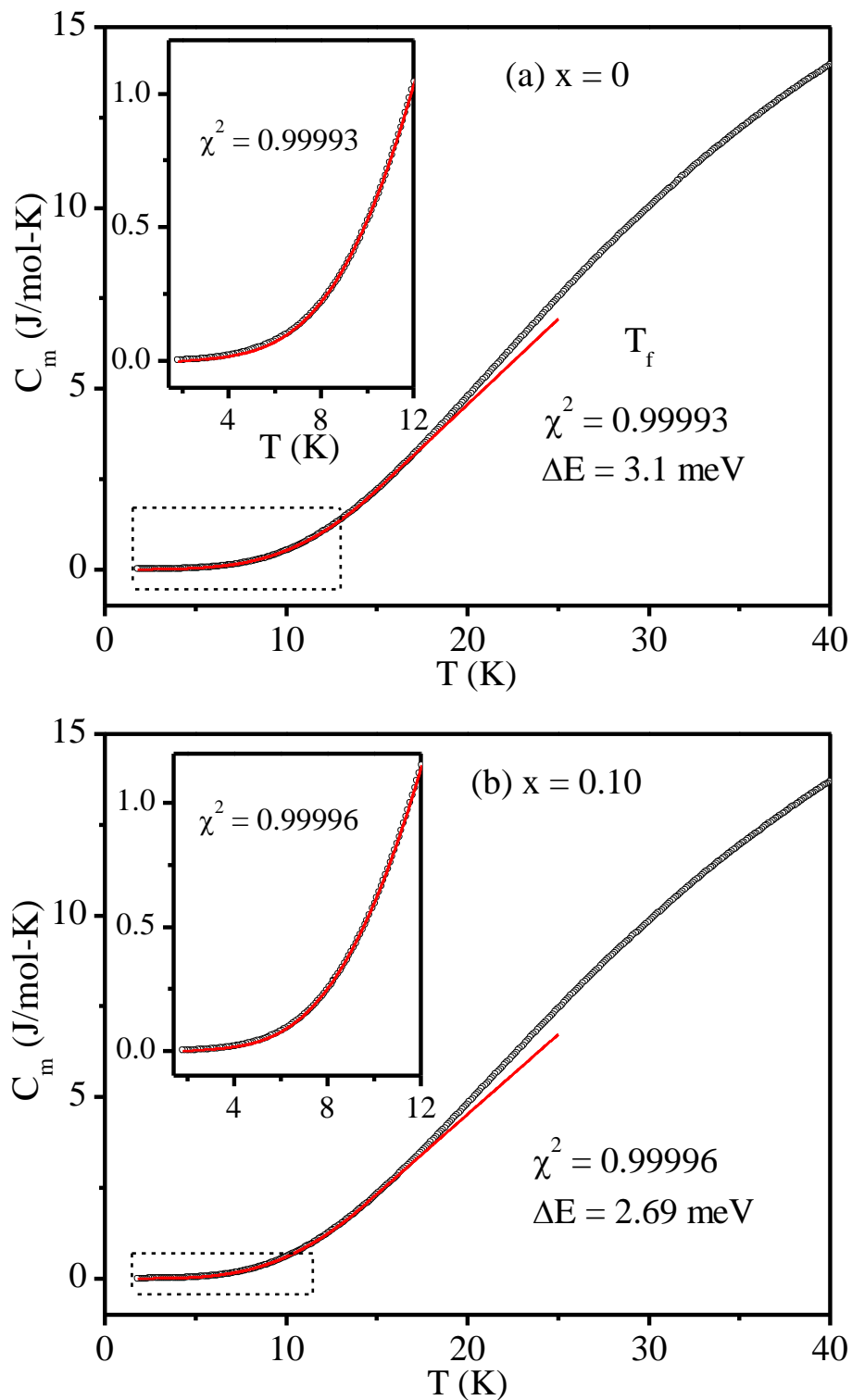


Figure 4.9: The fit to  $C_m$  vs  $T$  plot of BF-xBT using  $C_m = AT^3 + B\text{exp}(-\Delta E/k_B T)$  type function for (a)  $x = 0$ , (b)  $x = 0.10$ . The quality of the fits can be seen in the insets where a magnified view is plotted.

inelastic neutron scattering studies on BF ( $x=0$ ) [237] due to gapped magnons. We believe that many non-propagating gapped magnons contribute to the specific heat due to the coexisting spin glass phase because of which the inelastic peak shows an unusually large broadening. The experimental measured gap energy in specific heat and inelastic neutron scattering corresponds to some average value for several non-propagating magnons.

#### 4.4. Conclusions:

We have investigated the temperature dependence of specific heat ( $C_p$ ) in the temperature range 1.8 to 300K. Both the total specific heat and the magnetic contribution ( $C_m$ ) of BF- $x$ BT, obtained after subtracting phonon contributions, show the presence of a Boson peak in the  $C_p/T^3$  or  $C_m/T^3$  vs  $T$  plots whose peak temperature varies as  $T_{\text{Boson}} \sim (x - x_c)^{1/2}$  suggesting the possibility of a quantum critical point and  $x_c \sim 0.55$ . The magnetic specific heat ( $C_m$ ) below the Boson peak temperature cannot be explained without considering coexistence of spin glass and LRO AFM phases. It is shown that  $C_m$  in the temperature range 1.8 to 12 K is best described using a functional dependence  $C_m = AT^3 + B \exp(-\Delta E/k_B T)$  where the  $AT^3$  term is due to the long-range ordered (LRO) antiferromagnetic (AFM) phase and the exponential term is due to gapped magnons in the spin-glass (SG) phase. We believe that this is the first evidence for the coexistence of LRO and SG phases in concentrated systems using specific heat studies.

